

Inhomogeneous boundary conditions for Wannier–Mott excitons

N. N. Akhmediev, M. I. Sazhin, and A. V. Sel'kin

(Submitted 24 January 1989)

Zh. Eksp. Teor. Fiz. **96**, 720–734 (August 1989)

The specular reflection spectra of CdS crystals were determined at $T = 2$ K in the region of the $A_{n=1}$ exciton resonance. The great variability in the spectra could not be explained by the simple model of an exciton-free dead layer at the boundary of a crystal. Generalized boundary conditions were formulated for large excitons, which included inhomogeneous additional boundary conditions for the exciton polarization and inhomogeneous boundary conditions for the tangential component of the magnetic induction vector \mathbf{B} . An analysis of the energy balance equations at the surface of a crystal yielded further relationships among the parameters of the theory. The proposed system of boundary conditions described the case with a sharp internal boundary at the dead layer and allowed for the effects of the intrinsic and extrinsic mechanisms for formation of this layer. The reflection spectra of normally incident light were calculated numerically for various relationships among the parameters of the theory. New qualitative characteristics of the optical exciton reflection spectra were in good agreement with the experimental data.

1. INTRODUCTION

The extensive experimental and theoretical data already available make it possible to identify a number of general factors governing the formation of the exciton reflection spectra of light. The most important of these follow from the need to allow for the spatial dispersion and the associated problem of the boundary conditions, particularly supplementary boundary conditions.¹ In the case of Wannier–Mott excitons discussed in the present paper an important factor in determining the boundary conditions is an allowance for additional aspects of intrinsic nature such as the Coulomb potential of the images of electrons and holes² and the short-range contact interaction of an exciton with the surface of a sample, which alters the exciton energy and deforms its wave function near the surface of a crystal to a depth of the order of the exciton radius.^{3,4}

In real materials, in addition to the mechanisms of intrinsic nature, the exciton reflection spectra can also be affected significantly by extrinsic mechanisms due to surface layers with a chemical structure different from that in the interior, and also by the presence of defects and impurities located on the surface itself or in the surface layer.^{5–8} When the concentration of a charged impurity is sufficiently high, we can expect the internal electric field to contribute also.^{8,9}

Various theoretical approximations^{3,8–13} developed in recent years for the description of the optical exciton reflection spectra are usually difficult to apply in numerical calculations. Specific calculations of this kind have been limited mainly to the normal incidence of light and practically always yield satisfactory agreement with the experimental data. Naturally, such an agreement does not provide sufficient evidence to decide in favor of one specific theory.

The fullest experimental and theoretical analysis was provided by Hopfield and Thomas on the basis of a dead-layer model¹⁴ according to which the exciton contribution to the polarization P vanishes in a surface layer of thickness l of the order of the exciton radius, subject to the Pekar supplementary boundary condition¹⁵ $P = 0$ on the internal boundary of this layer. The dead layer model was confirmed by a number of experiments, including ellipsometric measure-

ments^{16,17} and experiments on oblique reflection of light.^{16,18,19} The dead layer model had been used successfully in an analysis of the experimental data on the reflection of light in the case of exciton resonances with a complex band structure^{20–24} including fine magneto-optic²³ and piezooptic²⁴ effects. The existence of a fairly abrupt internal boundary of the dead layer is supported also by independent experimental data on resonant elastic scattering of light from rough surfaces of the dead layer.²⁵

As far as the microscopic basis of the dead layer model is concerned, the initial interpretation provided by Hopfield and Thomas¹⁴ based on allowance solely for the image forces cannot be regarded as satisfactory. Subsequent investigations have shown that the contact interaction of an exciton with the surface^{3,4,26} and possibly a surface electric field^{8,9} may play a more important role in the formation of a dead layer. The combined effect of these factors⁹ and other difficult-to-control structural changes in a thin surface layer may result in a steep fall of the exciton contribution to the polarization near the surface and thus form a physical dead layer.

It should be pointed out that experimental deviations from the standard dead-layer model,¹⁴ which exist in the original samples²⁷ or are induced by external agencies (optical illumination, electron⁸ or ion²⁸ bombardment, etc.), are frequently observed. These observations confirm the participation of both intrinsic and extrinsic mechanisms in the formation of a dead layer. A natural generalization of the standard dead layer model¹⁴ is to formulate a more general system of boundary conditions on the internal surface of the dead layer.^{27,29,30} This system of the boundary conditions can be the set of inhomogeneous boundary conditions proposed in Refs. 1 and 31 and restated in a more general form in Ref. 32. An analysis of the reflection spectra on the basis of the boundary conditions of Refs. 1, 31, and 32 allowing for the presence of a dead layer has not yet been carried out.

Our aim will be to analyze the specular reflection spectra for normal incidence of light, calculated using a set of combined boundary conditions³¹ applicable to the experimental data obtained in the spectral region of the $A_{n=1}$ exci-

ton resonance in CdS crystals. These boundary conditions make it possible to describe the most important qualitative features of the reflection spectra, which cannot be reproduced by the standard Hopfield–Thomas model of a dead layer, and to account for the diversity of the exciton specular reflection spectra. The advantage of this method is its general validity and the relative simplicity in the sense of analytic procedures and numerical calculations, which makes it possible to generalize this theory further to more complex situations, including the case of oblique incidence of light.

In the next section we shall formulate a system with boundary conditions of the type suggested in Refs. 1 and 31 for Wannier–Mott excitons, generalized to the case of an absorbing medium, and we shall also discuss qualitatively the physical meaning of the parameters of the theory. In Sec. 3 the calculated theoretical curves will be compared with the experimental data on reflection from CdS crystals and new qualitative features of the spectra will be explained. A quantitative analysis of the parameters of the theory, which makes it possible to estimate possible spectral forms of the reflection curves, will be given in Sec. 4. The main results will be discussed in Sec. 5.

2. COMBINED ADDITIONAL BOUNDARY CONDITIONS IN THE DEAD-LAYER MODEL

We shall consider a narrow spectral interval $|\omega - \omega_0| \ll \omega_0$ in the vicinity of an isotropic isolated dipole-active exciton state with a resonant transition frequency ω_0 and we shall assume that the bulk of the investigated crystal is characterized by the permittivity¹

$$\varepsilon(\omega, k) = \varepsilon_b \left(1 + \frac{\omega_{LT}}{\omega_0 - \omega + \hbar k^2 / 2M - i\Gamma/2} \right), \quad (1)$$

where ω_{LT} is the longitudinal–transverse splitting, Γ is the damping parameter, ε_b is the background permittivity, and an explicit dependence of ε on k appears when the exciton translation mass M is finite, corresponding to an allowance for the spatial dispersion. A surface dead layer will be regarded as a homogeneous insulator of thickness l with a permittivity ε_l occupying a region $0 < z < l$ (where the $z = 0$ plane coincides with the external surface of the crystal). The additional boundary conditions for such a structure must be formulated on the internal boundary of the dead layer, i.e., at $z = l$ (Ref. 1). It is understood that there is a fairly thin (compared with the minimum wavelength) transition layer between the dead layer and the bulk of the crystal. In this case we can use the boundary-value problem in its classical formulation³³ and apply generalized boundary conditions^{1,31} which allow effectively for the properties of the transition region on the internal surface of the dead layer.

The external surface of the dead layer can be described by the classical system of Maxwell boundary conditions for the tangential components of the electric field \mathbf{E} and of the magnetic induction \mathbf{B} . On the internal surface of the dead layer, where the combined inhomogeneous additional boundary conditions are valid,^{1,31} the usual Maxwell boundary conditions are generally disobeyed. Surface exciton polarization currents \mathbf{j} induce a discontinuity of the tangential component of the vector \mathbf{B} (see Chap. 1, § 1 in Ref. 1). Therefore, the complete system of the boundary equations on the internal boundary of the dead layer ($z = l$) of interest to us becomes

$$[\mathbf{e}_z[\mathbf{B}(+0) - \mathbf{B}(-0)]] = \frac{4\pi}{c} \mathbf{j}_\parallel, \quad [\mathbf{e}_z[\mathbf{E}(+0) - \mathbf{E}(-0)]] = 0, \\ \mathbf{P}_\parallel + \frac{1}{k_0 T_\parallel} \frac{\partial \mathbf{P}_\parallel}{\partial z} = \frac{\xi_\parallel}{4\pi T_\parallel} \mathbf{E}_\parallel, \quad P_z + \frac{1}{k_0 T_\perp} \frac{\partial P_z}{\partial z} = \frac{\xi_\perp}{4\pi T_\perp} E_z, \quad (2)$$

where \mathbf{e}_z is a unit vector along the internal normal, and $\mathbf{P}_\parallel = \mathbf{P} - \mathbf{e}_z P_z$, $\mathbf{E}_\parallel = \mathbf{E} - \mathbf{e}_z E_z$, $k_0 = \omega/c$, T_\parallel , T_\perp , ξ_\parallel , ξ_\perp are the dimensionless phenomenological parameters, which are generally complex. These dimensionless parameters represent the diagonal components of second-rank tensors for which the off-diagonal elements vanish because of the symmetry of the problem. Using the energy balance at the interfaces, we can establish certain relationships among the parameters that occur in the boundary conditions described by Eq. (2) (Refs. 31, 34, 35). Following Ref. 35, the relationship between the densities of the energy fluxes on the internal $S(+0)$ and external $S(-0)$ surfaces of the interface ($z = l$) can be formulated as follows:

$$S(+0) = S(-0) - \frac{1}{4} \left\{ \mu \operatorname{Im} T_\parallel |T_\parallel| |P_\parallel|^2 + \left(\mathbf{j} \cdot + \frac{i\mu\xi_\parallel}{4\pi} \mathbf{P}_\parallel \cdot \right) \mathbf{E}_\parallel \right. \\ \left. + \mu \operatorname{Im} T_\perp |T_\perp| |P_z|^2 + \frac{i\mu\xi_\perp}{4\pi} P_z \cdot E_z \right\} - \frac{1}{4} \{ \text{c.c.} \}, \quad (3)$$

where $\mu = 2\pi k_0 \hbar \omega / \omega_{LT} \varepsilon_b M$. The parameters T_\parallel , T_\perp and ξ_\parallel , ξ_\perp are independent because of their different physical origin; the parameters T_\parallel and T_\perp are governed by the natural frequency and damping of excitons near the $z = l$ interface, whereas ξ_\perp , ξ_\parallel can be expressed in terms of the oscillator strength near this boundary and in fact allow for the difference between the effective electric field and the average field E (see § 10 in Ref. 1). Therefore, the terms in Eq. (3) containing the coefficients T_\parallel , T_\perp and ξ_\parallel , ξ_\perp , make independent contributions. The second and fourth terms in the braces should vanish because the field E is arbitrary. This circumstance determines the relationship between the polarization current and the exciton polarization at a boundary

$$\mathbf{j} = \frac{i\mu\xi_\parallel}{4\pi} \mathbf{P}_\parallel, \quad (4)$$

and also leads to the conclusion that $\xi_\perp = 0$. In the first and third terms the imaginary parts obey $\operatorname{Im} T_\parallel \geq 0$ and $\operatorname{Im} T_\perp \geq 0$ (Ref. 35).

The above system of the boundary conditions can be used to calculate the spectra of light incident normally or obliquely. In this case the boundary conditions allow solely for the tangential component \mathbf{j}_\parallel of the surface current \mathbf{j} . We can generalize this system of boundary conditions even further by allowing for the normal component \mathbf{j}_z of the current \mathbf{j} , which may be associated with a discontinuity of the tangential component of the field E at the boundary in question. The generalized boundary conditions proposed in Ref. 32 for the normal incidence of light allow for this possibility. In the case of oblique incidence of light when $\mathbf{j}_z \neq 0$, the parameter ξ_\perp should also differ from 0. In the subsequent interpretation of the experimental data we shall confine ourselves to the case of the normal incidence of light when only the parameters ξ_\parallel and T_\parallel are important. It should be noted that in the case of the normal incidence of light our model of a “generalized” dead layer is formally equivalent to the model of a zero-radius surface potential³⁶ when the dead layer is allowed for effectively in the boundary conditions.

3. ANOMALIES IN THE EXCITON REFLECTION SPECTRA: EXPERIMENTS AND THEORETICAL CALCULATIONS

We investigated experimentally cadmium sulfide single-crystal platelets grown by the gas-transport method.¹⁾ We determined the reflection spectra for natural faces of these crystals without any special treatment. We limited ourselves to the experimental geometry in which the reflecting face of a crystal was parallel to the optic axis c of the crystal and light with the $E \perp c$ polarization propagated along the $k \perp c$ direction at a near-normal ($\varphi \sim 8^\circ$) angle of incidence. These crystals were immersed directly in pumped-out liquid helium at $T = 2$ K and the spectra were recorded using a DFS-24 spectrometer in the region of the lowest exciton resonance $A_{n=1}$ of CdS crystals. The spectral composition of light incident on the crystal was limited to the interval 2.540–2.577 eV, which was outside the interband absorption region. This was important in view of the extreme sensitivity of the specular reflection spectra to illumination corresponding to the fundamental absorption region.³⁷

Our experimental investigation of about 150 crystalline samples established that the specular reflection spectra of

some CdS crystals differed considerably from one another even in the qualitative sense. This difference appeared in spite of the fact that crystals were grown by the same method and were clearly due to variations in the technological parameters of the growth process that were difficult to control. It should be pointed out that the majority of the samples (in excess of 80%) exhibited spectra of the standard type reported in Refs. 14, 19, and 37 which could be interpreted using the "classical" dead-layer model proposed by Hopfield and Thomas.¹⁴

Figure 1a shows the experimentally recorded specular reflection spectra of several crystals (1–7) which had certain characteristic features. The most frequent of these was a spectrum (1) with a small kink at a frequency ω_L and a reflection minimum on the long-wavelength side of ω_L . In spectrum (2) the kink was clearly defined, and it was manifested even more strikingly in the spectrum labeled 3. These strong features were absent from spectrum 4, whereas spectra 5 and 6 feature the frequency ω_L called a spike in Ref. 14. A distinguishing characteristic of spectra 5 and 6 was that the absolute reflection minima in these spectra were located

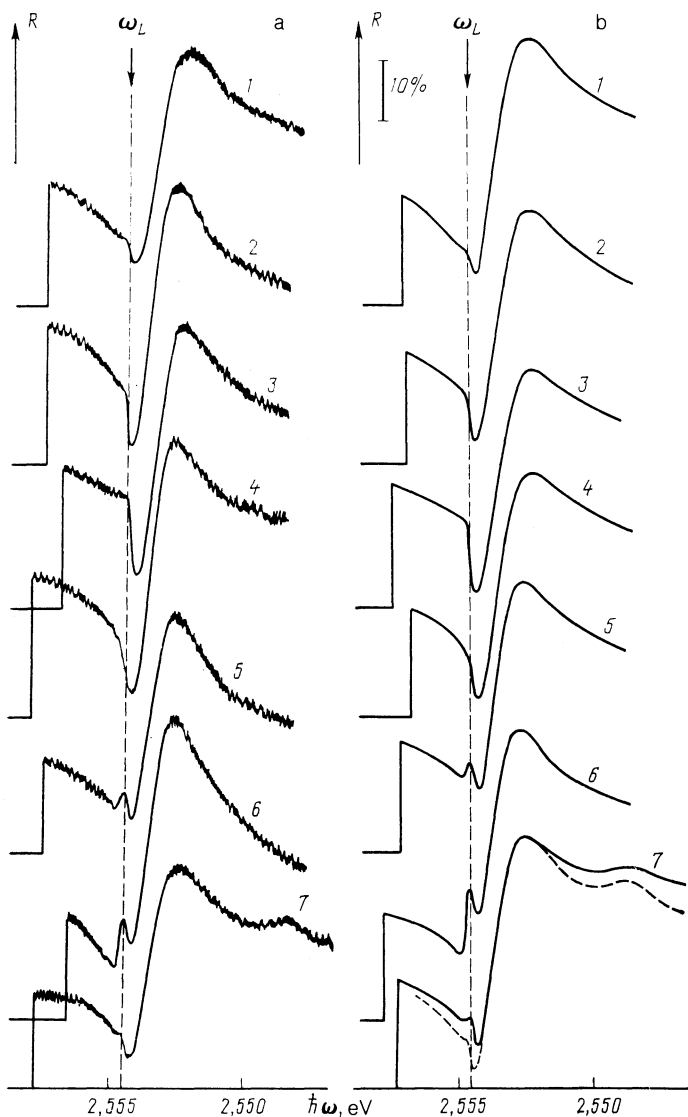


FIG. 1. Comparison of the experimental specular reflection spectra (a) of CdS crystals ($T = 2$ K, $A_{n=1}$ exciton, angle of incidence $\varphi \approx 8^\circ$, polarization of light $E \perp c$) with the results of a theoretical calculation (b) carried out using the generalized exciton-free dead-layer model in the case of normal incidence of light. The spectra in Fig. 1a were obtained for samples with natural growth faces, whereas the theoretical curves (b) were calculated for the parameters listed in Table I and in the text.

TABLE I. Values of the parameters used in calculations of the theoretical (continuous) curves in Fig. 1b (parameters for the dashed curve are given in the text).

Curve No.	ξ_{\parallel}	$\text{Im } T_{\parallel}$	$\hbar\Gamma$, meV	Values of parameters common to continuous curves 1–7
1	40	80	0,1	$\hbar\omega_0=2,5524$ eV $\hbar\omega_{LTS}=2$ meV $\varepsilon_b=\varepsilon_l=9,3$ $M=0,9m_0$ (m_0 is the mass of a free electron) $l=70$ Å $\text{Im } \xi_{\parallel}=0$ $\text{Re } T_{\parallel}=22,0$
2	80	30	0,1	
3	100	12	0,09	
4	80	20	0,15	
5	26	12	0,09	
6	-6	10	0,05	
7	12	5	0,15	

on opposite sides of the frequency ω_L , and in each case the spike was asymmetric. In spectrum 7, we found not only characteristic features at the frequency ω_L , but also an additional small maximum on the long-wavelength side of the main one. In the case of crystals not subjected to a special treatment (chemical etching, electron or ion bombardment, strong laser illumination, etc.) the spectra 1–7 represented the full range of qualitative spectral features. Illumination with moderately strong ultraviolet radiation sometimes transformed spectrum 7 into spectrum 5 and then into spectrum 6.

We analyzed the experimental data using the above theory and the parameters of the boundary conditions of Eq. (2) variable within the wide limits permitted by the inequality $S_z(+0) \leq S_z(-0)$. The main parameters of the standard dead-layer model, including the bulk parameters of excitons, have in fact remained constant. It was found that the main spectral features could be reproduced in the calculations even if the parameters of the boundary conditions ξ_{\parallel} and T_{\parallel} were altered. It was sufficient to consider the real values of ξ_{\parallel} , which corresponded to a change in the oscillator strength of the transition and in the effective mass of an exciton in the boundary layer, as demonstrated in Refs. 1 and 36 on the basis of model considerations.

Figure 1b shows the spectra (continuous curves 1–7) calculated for the parameters listed in Table I. It should be pointed out that the theoretical spectrum 1 corresponds in practice to the Pekar supplementary boundary conditions¹⁵ on the internal boundary of the dead layer. An increase in the reflection coefficient at the kink at the frequency ω_L in the theoretical spectra 2 and 3, relative to the main minimum, is due to an increase in ξ_{\parallel} and a simultaneous reduction in $\text{Im } T_{\parallel}$. The kink flattens out as Γ is increased (curve 4). A reduction in Γ gives rise to a spike at the kink and the spike asymmetry depends on the absolute value and sign of ξ_{\parallel} (compare curves 4, 5, and 6).

Reduction in $\text{Im } T_{\parallel}$ in the long-wavelength part of the spectrum gives rise to a maximum at a position governed by the value of $\text{Re } T_{\parallel}$. In agreement with the experimental curve 7, we have to assume $\text{Re } T_{\parallel} = 22$. We used the same value of $\text{Re } T_{\parallel}$ in calculations of all the other theoretical curves allowing for the fact that the spectral position of the additional long-wavelength maximum of the experimental curves is stable. An increase in $\text{Re } T_{\parallel}$ is accompanied by a shift of the additional maximum in the theoretical spectrum 7 toward longer wavelengths.

The physical reason for the additional weak maximum in the type-7 reflection spectrum may also be the excitation

of an exciton bound to a surface neutral center.³⁸ Such a situation can be described qualitatively using our approach involving introduction of an additional resonance in the dead layer on the assumption that

$$\varepsilon_l(\omega) = \varepsilon_b + \frac{\varepsilon_b \omega_{LTS}}{\omega_s - \omega - i\Gamma_s/2},$$

where ω_s is the resonance frequency of a surface oscillator, ω_{LTS} is the effective longitudinal–transverse splitting (*LTS*), and Γ_s is the damping constant of a surface oscillator. Good agreement with the experimental results is obtained on the assumption that $\hbar(\omega_0 - \omega_s) = 3.88$ meV, $\hbar\omega_{LTS} = 0.2$ meV, $\hbar\Gamma_s = 0.85$ meV, $\varepsilon_b = 10$, $\hbar\Gamma = 0.075$ meV, and $1/T_{\parallel} = \xi_{\parallel} = 0$. The values of the other bulk parameters are given on the right-hand side of Table I. The results of the corresponding theoretical calculation are presented in Fig. 1b in the form of the dashed curve labeled 7. It follows from this comparison of the theory and experiment that the model of a surface oscillator in a dead layer better describes the experimental situation.

On the whole, our method of generalized boundary conditions makes it possible to reproduce in detail practically all the experimental features of the observed reflection spectra without specifying the exciton surface potential, which has undoubted advantages over other familiar methods. This is particularly important when we are allowing for real insufficiently controlled mechanisms of formation of a thin transition layer near the crystal surface.

The experimental spectra shown in Fig. 1a were obtained for samples grown under approximately identical technological conditions. The samples displaying type-1 spectra for near-normal incidence of light on the boundary of a crystal had been the subject of earlier very thorough and comprehensive investigations, including studies of specular reflection of light with different polarizations incident obliquely and corresponding to the *A* (Refs. 16 and 19) and *B* (Refs. 21 and 22) exciton resonances, as well as high-sensitivity ellipsometric measurements¹⁶ and a study of resonant diffuse reflection of light.²⁵ The standard dead layer model¹⁴ provided not only qualitative but also very good quantitative theoretical descriptions of the great variety of defects observed in these investigations. The existence of an exciton-free dead layer with a sharp boundary is of fundamental importance for the formation of the observed resonance exciton spectra, including the spectra of surface modes.³⁹

There is at present no serious evidence in support of other possible explanations of the wide range of resonances typical of samples with type-1 reflection spectra. The validity of any alternative model can be judged only if this model

is used to provide a quantitative description of all the experimental results mentioned above, not just the specular reflection spectra obtained for normal incidence of light, as is done in the majority of the published investigations.

In view of the similar technological conditions during growth of the samples exhibiting spectra 1–7 in Fig. 1a, introduction of the generalized dead-layer model is fully justified. The good agreement between the theoretical curves in Fig. 1b and the experimental spectra in Fig. 1a confirms the validity and effectiveness of this approach.

4. PARAMETERS OF THE BOUNDARY CONDITIONS AND THE REFLECTION SPECTRA NEAR EXCITON RESONANCES

A fairly frequent feature of the specular reflection spectra recorded in the region of the $A_{n=1}$ exciton resonance of CdS crystals is a spike representing a sharp peak at the frequency ω_L (curves 6 and 7 in Fig. 1a). If the boundary between the dead layer and the bulk of the sample is sufficiently abrupt and the dissipative damping is sufficiently weak (which is typical of the cases discussed), the appearance of a spike at the frequency ω_L is of fundamental importance because this spike is related to the threshold nature of multi-channel scattering of the incident light wave. As the energy of the incident photon at the frequency ω_L increases, polaritons from the additional (known as the upper) branch begin to participate in energy transfer. In the case of oblique incidence the threshold frequency ω_t shifts in accordance with the law

$$k_2(\omega_t)/k_0 = \sin \varphi,$$

where φ is the angle of incidence and k_2 is the wave vector of an upper-branch polariton.³⁷ The appearance of a kink at the frequency ω_L in the spectra labeled 1–3 is due to the same threshold effect. The actual profiles of the threshold features depend on the values of parameters occurring in the boundary conditions.

The spectra 6 and 7 in Fig. 1 exhibit clearly an asymmetry of the spikes, which is of different nature for different values of the parameters (Fig. 1b, Table I). These parameters may vary within wide limits but the qualitative profile of a spike is retained. Figure 2 shows the complex plane of the variable T_{\parallel} (plotted bearing in mind that $\text{Im } T_{\parallel} \geq 0$) where the points lying on curves labeled 1 ($\xi_{\parallel} = 40$), 2 ($\xi_{\parallel} = 0$), and 3 ($\xi_{\parallel} = -40$), plotted on the assumption that $\hbar\Gamma = 0.075$ meV and for fixed values of the other parameters (see the right-hand part of Table I), represent the symmetric form of the spike (inset b in Fig. 2). The inner regions bounded by curves 1–3 and the abscissa determine the range of an asymmetric spike of type c (inset c); an asymmetric spike of type a (inset a) appears in the parts of the T plane which are outside curves 1–3. In these regions an increase in T_{\parallel} gives rise to a situation described by a system of boundary conditions corresponding to the standard dead layer model with the Pekar additional boundary conditions.¹⁵

It is clear from Fig. 2 that points on the plane

$$T_{\parallel} = \text{Re } T_{\parallel} + i \text{Im } T_{\parallel}$$

may describe qualitatively different types of asymmetry of a spike, depending on the value of ξ_{\parallel} . The change in the nature of the spike asymmetry need not be accompanied by a

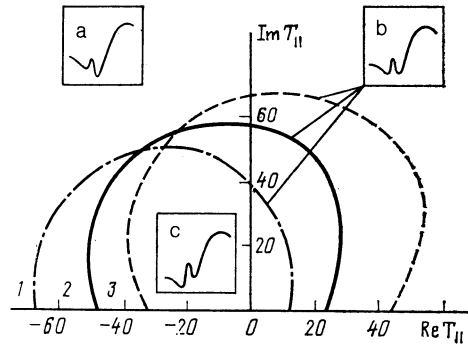


FIG. 2. Values of the complex parameter T_{\parallel} which ensure the appearance of a symmetric spike (inset b) in the specular reflection spectrum of normally incident light: $\xi_{\parallel} = 40$ (curve 1), 0 (curve 2), -40 (curve 3); $\hbar\Gamma = 0.075$ meV; the values of the other parameters are listed in Table I. The internal regions bounded by curves 1–3 and the abscissa correspond to an asymmetric spike of type c (inset c), whereas an asymmetric spike of type a (inset a) appears in regions external to curves 1–3.

change in the sign of ξ_{\parallel} , as is true in the specific case of curves 6 and 7 in Fig. 1b. The qualitative profile of a spike changes when the position of a point on the T_{\parallel} plane changes relative to the curve representing a constant value of ξ_{\parallel} : when the point goes over from the outer to the inner region or vice versa. This may occur as a result of a change in the value of ξ_{\parallel} or in the value of T_{\parallel} .

In the spectra shown in Fig. 1 we concentrated our attention on the features which appear near the frequency ω_L . The parameters of the theory were varied in relatively narrow ranges (Table I) which made it possible to describe our experimental spectra. The real part of the parameter T had the value shown in Table II, so that it was possible to reproduce qualitatively the long-wavelength maximum in the specular reflection spectra, which appeared sometimes in the spectra of CdS at 2.5485 eV (curves labeled 7 in Fig. 1). In view of the general nature of our approach, it would be of interest to calculate the specular reflection spectra for values of the parameters which are variable within wide limits. The results of such a calculation could be of importance in the interpretation of the experimental data in those cases when the profile of the observed specular reflection spectrum differs from the spectra shown in Fig. 1.

Curves 1–10 in Fig. 3 demonstrate the possible spectral dependence of the reflection coefficient of light incident normally on a sample with a dead layer. It is worth noting an additional structure in the spectra, which appears at moderately large values of $|T_{\parallel}|$. In the case of curve 1 it is manifested by a clear dispersion structure near the energy $\hbar\omega \approx 2.551$ eV, whereas in the case of curves 3–4 it is located closer to the frequency ω_L and exhibits antidispersive (reversed) behavior. As $\text{Re } T_{\parallel}$ decreases, the structure shifts toward shorter wavelengths and becomes localized near the resonance frequency ω_0 , where $\text{Re } T_{\parallel} = 0$. Further reduction of $\text{Re } T_{\parallel}$ in the range of negative values shifts the structure gradually toward the frequency ω_L , but remains always on the long-wavelength side of ω_L . In the limit $|T_{\parallel}| \rightarrow \infty$ when the finite value of ξ_{\parallel} remains fixed, we have the standard dead-layer model.¹⁴

Curves 6–9 in Fig. 3 correspond to the case when the surface polarization displacement current j_{\parallel} influences sig-

TABLE II. Values of parameters used in calculations of the theoretical curves plotted in Fig. 3.

Curve No.	ξ_{\parallel}	$\text{Re } eT_{\parallel}$	$\text{Im } T_{\parallel}$	Comments
1	150	13	0	Values of $\hbar\omega_0$, $\hbar\omega_{LT}$, ϵ_v , ϵ_L and M are listed in Table I; $l = 70 \text{ \AA}$ and $\hbar\Gamma = 0.075 \text{ meV}$ for curves 1-9; $l = 124 \text{ \AA}$ and $\hbar\Gamma = 0.09 \text{ meV}$ for curve 10
2	420	4	0	
3	420	0	0	
4	420	-8	0	
5	420	-62	0	
6	1000	100	0	
7	-1000	100	0	
8	1000	0	100	
9	-1000	0	100	
10	180	22	38	

nificantly the reflection spectrum because the values of ξ_{\parallel} are anomalously large. The minimum value of the reflection coefficient R represents a few tens of percent, and the maximum value of R (curve 7) can reach nearly 100%. Curve 10 also corresponds to a fairly large value of ξ_{\parallel} , but it was calculated using a somewhat overestimated thickness of the dead layer ($l = 124 \text{ \AA}$). This curve is interesting because it reproduces all the qualitative features of the experimental reflection spectrum reported in Ref. 27, where a satisfactory agreement between the experimental results and the dead layer model with a homogeneous set of the supplementary boundary conditions ($\xi_{\parallel} = 0$) was not achieved.

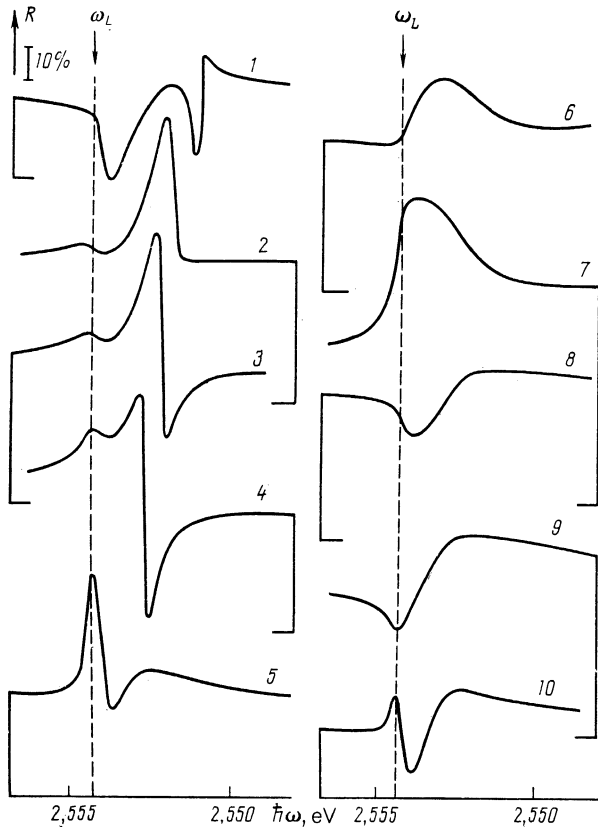


FIG. 3. Specular reflection spectra in the exciton resonance region calculated using the generalized dead-layer model for bulk parameters typical of CdS crystals ($A_{n=1}$ exciton). The parameters in the boundary conditions are listed in Table II.

5. DISCUSSION OF RESULTS

For the normal incidence of light on a dead layer, Eq. (2) contains in fact only three parameters $\text{Re } T_{\parallel}$, $\text{Im } T_{\parallel}$, and ξ_{\parallel} . The selection of the real value of ξ_{\parallel} follows from the physical meaning of this parameter, which is a quantity associated with the effective oscillator strength in the transition layer (see § 10 in Ref. 1). In the case of the complex parameter T_{\parallel} , its real part $\text{Re } T_{\parallel}$ represents a shift of a certain effective resonant frequency in the transition layer and possibly a change in the effective mass of the exciton. The imaginary part, $\text{Im } T_{\parallel}$, governs the energy dissipation in the same transition layer.³⁵ From the point of view of the theory of scattering by a zero-radius potential the real quantity $(k_0 T_{\parallel})^{-1}$ may be regarded formally as a generalized scattering length, corresponding either to a bound surface state ($\text{Re } T_{\parallel} > 0$) or to a "virtual" surface level ($\text{Re } T_{\parallel} < 0$).³⁶

It follows from calculations (Fig. 3) that $\text{Re } T_{\parallel}$ governs the spectral position of the additional long-wavelength structure of the reflection coefficient. If $\Gamma \rightarrow 0$ and $\text{Im } T_{\parallel} \rightarrow 0$, then at some frequency $\omega'_i \ll \omega_L$, where such a structure appears, the reflection of light amounts to 100% indicating the absence of energy transfer into the investigated crystal at this frequency. Bearing in mind that in the region $\omega \ll \omega_L$ when $\Gamma = 0$ only a polariton mode from the "lower" dispersion branch 1 is propagated and the absence of energy transfer at the frequency ω'_i should be regarded as complete suppression of the mode 1 at this frequency. In that sense the frequency ω'_i can be regarded as equivalent to ω_i (see Sec. 4) and it represents a threshold for the scattering of the incident light wave.

It follows from the additional boundary conditions of Eq. (2) that \mathbf{P}_{\parallel} yields directly a relationship between the amplitudes $\mathbf{E}_{\parallel}^{(1)}$ and $\mathbf{E}_{\parallel}^{(2)}$ of the normal modes 1 and 2 on the internal surface of the dead layer

$$\sum_{j=1}^2 \alpha_j \mathbf{E}_{\parallel}^{(j)} = 0, \quad \alpha_j = (T_{\parallel} + in_j)(n_j^2 - \epsilon_b) - \xi_{\parallel}, \quad (5)$$

where n_j is the refractive index of the j th mode. Suppression of the mode 1 occurs for $\alpha_2 = 0$, i.e., when

$$T_{\parallel} = -in_2 + \xi_{\parallel} / (n_2^2 - \epsilon_b). \quad (6)$$

This expression governs, via $n_2(\omega)$, the threshold frequency ω'_i at fixed values of T_{\parallel} and ξ_{\parallel} . It is obeyed rigorously if $\Gamma = 0$ in the spectral range $\omega \ll \omega_L$, where $\text{Re } n_2 = 0$ and it

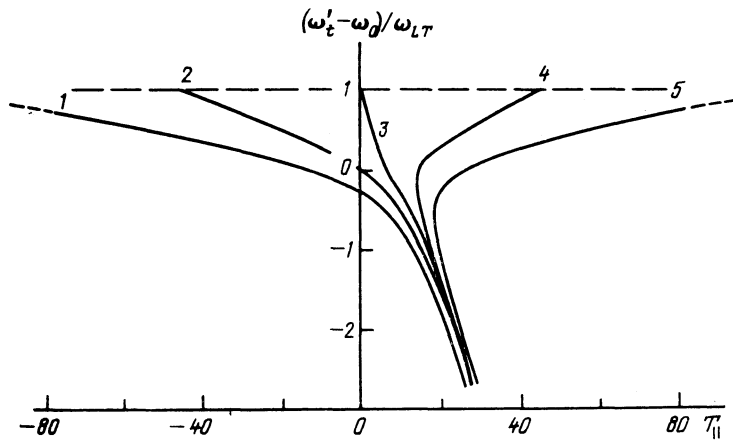


FIG. 4. Dependence of the threshold frequency ω'_t [in units of $(\omega'_t - \omega_0)/\omega_{LT}$], at which an additional long-wavelength structure appears in the reflection spectrum, on the parameter T_{\parallel} when $\text{Im } T_{\parallel}; \xi_{\parallel} = 1000$ (1), 420 (2), 0 (3), -420 (4), and -1000 (5). The values of the bulk parameters typical of CdS ($A_{n=1}$ exciton) are shown on the right-hand side of Table I ($\hbar\Gamma = 10^{-3}$ meV).

corresponds to the real values of T_{\parallel} . Allowance for the dissipative damping ($\Gamma > 0$, $\text{Im } T > 0$) means that the condition (6) cannot be satisfied exactly so that when Γ or $\text{Im } T_{\parallel}$ increases, the spectral features in the region of the frequency ω'_t are gradually flattened out and then disappear. Obviously, the short-wavelength limit of the spectral shift of the threshold frequency ω'_t is governed by the condition $n_2 = 0$, i.e., we have $\omega'_t = \omega_L$, which corresponds to the value $T_{\parallel} = -\xi_{\parallel}/\epsilon_s$.

Figure 4 shows the dependence of the threshold frequency ω'_t on the parameter T_{\parallel} for several fixed values of ξ_{\parallel} (given in the caption of Fig. 4) and the bulk parameters typical of the $A_{n=1}$ exciton resonance in CdS crystals (right-hand side of Table I). Trace 3 corresponds to a situation with a surface mechanical exciton characterized by $\xi_{\parallel} = 0$ and discussed earlier.^{8,36} Traces 1 and 2 are plotted for $\xi_{\parallel} > 0$, whereas traces 4 and 5 are plotted for $\xi_{\parallel} < 0$. Trace 2 describes a shift of the threshold singularity ω'_t in the spectra 2-5 in Fig. 3 ($\xi_{\parallel} = 420$). It is clear from the functions labeled 4 and 5 that in the range of negative values of ξ_{\parallel} and some fixed values of T_{\parallel} a polariton mode 1 may be suppressed simultaneously at two threshold frequencies.

An analysis of the experimental results given above and the conclusions of many earlier investigations discussed earlier suggest that a dead layer of thickness l of the order of 2-3 exciton radii and with an exciton-free core is indeed formed near the surface of a crystal. A thin transition region of thickness $\Delta l \ll \lambda$, where λ is the minimum length of the excited normal mode, exists between the internal boundary of the dead layer and the bulk of a crystal. Within this thin layer the exciton polarization \mathbf{P} , and also the fields \mathbf{E} and \mathbf{B} , may behave singularly. In particular, the appearance of the surface polarization displacement \mathbf{j} is one of the manifestations of such a singularity.

In the case of CdS crystals with natural growth faces, which were not subjected to any additional treatment, we found that $\Delta l < l \leq 100 \text{ \AA}$, which is a small quantity compared with the characteristic absorption length $\alpha^{-1} \approx 1000 \text{ \AA}$ in the exciton resonance region. This is in good agreement with the observation in CdS of very narrow (with very weak inhomogeneous broadening) Brillouin scattering lines⁴⁰ and with the narrow A_L line due to a mixed mode. The condition $\Delta l \ll \alpha^{-1}$ is necessary also for the explanation of the experi-

mentally observed small shift of the spike (the central singularity near the frequency ω_L) in the inclined reflection spectra observed when the angle of incidence is increased.³⁷

The thickness l of the investigated dead layer corresponds to the range of action of the nonadiabatic exciton potential^{3,13} (where the internal motion of an electron and a hole in an exciton ceases to be independent of the center-of-mass motion). Such a potential may form as a result of the combined effect of intrinsic and extrinsic mechanisms. In particular, an extrinsic Stark reduction in the exciton energy in a surface electric field, corresponding to bending of the electron and hole energy bands at the surface, may compensate partly an intrinsic increase in the energy⁹ and reduce the thickness of the transition layer by Δl .

An intrinsic mechanism for the formation of the dead layer can be ignored completely in the case of a strong surface electric field which ionizes an exciton at a distance l on the order of 2-3 exciton radii from the surface. This is exactly the situation that can benefit from a calculation of the reflection spectra in the adiabatic approximation used in Ref. 8 for the Schottky barrier model.

The Schottky model makes it possible to estimate roughly the influence of a surface electric field $E(z)$ on the behavior of an exciton. If w is the thickness of the space charge layer with an excess concentration of charged donors $N^+ = N_p - N_A$ (in the case of an n -type semiconductor such as CdS), ϵ_s is the static permittivity, and e is the absolute value of the electron charge, then under thermodynamic equilibrium conditions at low temperatures we have

$$E(z) = (4\pi e/\epsilon_s)N^+(z-w)$$

in the range of depths $0 \leq z \leq w$ and

$$E(z) = 0$$

outside this range. The intrinsic mechanism ceases to operate when $|E(l)| \gtrsim E_I$, where E_I is the absolute value of the ionizing field (for the $A_{n=1}$ exciton in CdS this field is $E_I \sim 10^5 \text{ V/cm}$), which corresponds to the inequality

$$N^+|l-w| \gtrsim E_I \epsilon_s / 4\pi e.$$

For typical values $N^+ \lesssim N_D \sim 10^{15} \text{ cm}^{-3}$ in our CdS samples the above inequality may be satisfied only if w is sufficiently large ($w \gtrsim 5 \times 10^4 \text{ \AA}$). Throughout the part of

the crystal where a reflected wave can form (whose thickness is of the order of $\alpha^{-1} \sim 10^3 \text{ \AA}$) in practice the field retains ionizing intensity [$|E(\alpha^{-1})| \approx (1 - \alpha^{-1}/w)E_I$], which should destroy the structure in the reflection spectrum. This is why we cannot use the adiabatic approach of Ref. 8 to describe our experimental results.

The value of the electric field $|E(l)|$, in which the boundary condition method can be applied, can vary within wide limits depending on the characteristic values of ω . If $w \gtrsim \alpha^{-1}$, the field $E(l)$ should be much weaker than E_I . If the distance (depth) w is comparable with l , then $|E(l)|$ may even exceed E_I . The parameters occurring in the boundary conditions should then be sensitive to the actual distribution of the built-in charge N^+ , which can be controlled by external factors.

6. CONCLUSIONS

The approach to the solution of the problem of reflection of light in the spectral region of exciton resonances adopted above is of fairly general validity. There is no need to specify completely the model from the microscopic point of view, but the model should reflect the principal features of the behavior of an exciton near the crystal surface. A generalized model of an exciton-free surface dead layer has been developed on the basis of this approach, where it is assumed that this layer may form as a result of intrinsic or extrinsic mechanisms. Such a layer represents a homogeneous surface region of a crystal of thickness amounting to 2–3 exciton radii, which makes no exciton contribution to the polarization. The internal boundary of this region is subject to inhomogeneous supplementary boundary conditions imposed on the exciton polarization. The parameters of these conditions allow effectively for the changes in the resonance frequency, dissipative damping, and effective mass of excitons, as well as for a change in the oscillator strength of the transition in a thin transition region between the dead layer and the bulk of the crystal.

Variation of the values of three parameters of the supplementary boundary conditions makes it possible to describe theoretically the fundamental features of the experimentally observed exciton reflection spectra of light incident on CdS crystals and demonstrates, in agreement with the experimental data, the great variety of possible reflection spectra. Calculations of these spectra on the basis of the generalized dead layer model with inhomogeneous supplementary boundary conditions predicts new spectral features which appear for a certain selection of the parameters of the additional boundary conditions and which we observed in the case of CdS and other semiconductor crystals in the spectral region of large exciton states.

The detailed structure of the transition region near the surface in a real crystal depends on many difficult-to-control factors, particularly the technological conditions during the growth of crystals. A self-consistent microscopic analysis of the behavior of an exciton in this situation is a very difficult and cumbersome task. The solution of this problem is not always justified from the practical point of view, particularly when an analysis is made of other (apart from specular reflection) optical resonances associated with allowance for the influence of interfaces on the scattering of light by a rough surface, for luminescence due to bulk polaritons, for

resonant elastic and inelastic bulk scattering of light, for emission of radiation, and for scattering accompanied by the excitation of surface polaritons. In this respect the method of inhomogeneous boundary conditions developed above provides a very effective and practical method for solving problems relating to surface effects which are important from the physical point of view.

¹¹The authors are grateful to Sv. A. Pendyur and O. N. Talenskii for supplying crystal samples.

¹V. M. Agranovich and V. L. Ginzburg, *Spatial Dispersion in Crystal Optics and the Theory of Excitons*, Wiley, New York (1967).

²S. Sakoda, *J. Phys. Soc. Jpn.* **40**, 152 (1976).

³A. D'Andrea and R. Del Sole, *Phys. Rev. B* **25**, 3714 (1982).

⁴S. Satpathy, *Phys. Rev. B* **28**, 4585 (1983).

⁵N. A. Davydova, É. N. Myasnikov, and M. I. Strashnikova, *Fiz. Tverd. Tela (Leningrad)* **15**, 3332 (1973) [*Sov. Phys. Solid State* **15**, 2217 (1974)].

⁶F. Evangelisti, A. Fropa, and F. Patella, *Phys. Rev. B* **10**, 4253 (1974).

⁷I. Munder, R. Helbig, and J. Lagois, *Solid State Commun.* **41**, 553 (1982).

⁸V. A. Kiselev, B. V. Novikov, and A. E. Cherednichenko, *Exciton Spectroscopy of Surface Layers of Semiconductors* [in Russian], Leningrad State University (1987).

⁹L. Schultheis and I. Balslev, *Phys. Rev. B* **28**, 2292 (1983).

¹⁰A. Stahl, *Phys. Status Solidi B* **106**, 575 (1981).

¹¹A. Stahl and I. Balslev, *Electrodynamics of the Semiconductor Band Edge*, Springer Verlag, Berlin (1987) [Springer Tracts in Modern Physics, Vol. 110].

¹²L. Gotthard, A. Stahl, G. Czajkowski, *J. Phys. C* **17**, 4865 (1984).

¹³S. Inoue and M. Nakayama, *J. Phys. Soc. Jpn.* **56**, 2174 (1987).

¹⁴J. J. Hopfield and D. G. Thomas, *Phys. Rev.* **132**, 563 (1963).

¹⁵S. I. Pekar, *Zh. Eksp. Teor. Fiz.* **33**, 1022 (1957) [*Sov. Phys. JETP* **6**, 785 (1958)].

¹⁶A. B. Pevtsov and A. V. Sel'kin, *Ellipsometry: Theory, Methods, Applications* [in Russian], ed. by A. V. Rzhaznov and L. A. Il'in, Nauka, Novosibirsk (1987), p. 156.

¹⁷S. B. Moskovskii and L. E. Solov'ev, *Zh. Eksp. Teor. Fiz.* **86**, 1419 (1984) [*Sov. Phys. JETP* **59**, 831 (1984)].

¹⁸I. Broser, M. Rosenzweig, R. Broser, M. Richard, and E. Birkicht, *Phys. Status Solidi B* **90**, 77 (1978).

¹⁹A. B. Pevtsov and A. V. Sel'kin, *Zh. Eksp. Teor. Fiz.* **83**, 516 (1982) [*Sov. Phys. JETP* **56**, 282 (1982)].

²⁰G. D. Mahan and J. J. Hopfield, *Phys. Rev.* **135**, A428 (1964).

²¹E. L. Ivchenko and A. V. Sel'kin, *Zh. Eksp. Teor. Fiz.* **76**, 1837 (1979) [*Sov. Phys. JETP* **49**, 933 (1979)].

²²A. B. Pevtsov and A. V. Sel'kin, *Fiz. Tverd. Tela (Leningrad)* **25**, 157 (1983) [*Sov. Phys. Solid State* **25**, 85 (1983)].

²³M. Rosenzweig, *Phys. Status Solidi B* **129**, 187 (1985).

²⁴H. Mathieu, Y. Chen, J. Camassel, J. Allegre, and D. S. Robertson, *Phys. Rev. B* **32**, 4042 (1985).

²⁵V. A. Kosobukin, and A. V. Sel'kin, *Solid State Commun.* **66**, 313 (1988).

²⁶I. Balslev, *Phys. Status Solidi B* **88**, 155 (1978).

²⁷F. Patella, F. Evangelisti, and M. Capizzi, *Solid State Commun.* **20**, 23 (1976).

²⁸V. A. Zuev, D. V. Korbutyak, M. V. Kurik, V. G. Litovchenko, A. Kh. Rozhko, and P. A. Skubenko, *Pis'ma Zh. Eksp. Teor. Fiz.* **26**, 455 (1977) [*JETP Lett.* **26**, 327 (1977)].

²⁹R. Monreal, F. Garcia-Moliner, and F. Flores, *Solid State Commun.* **32**, 613 (1979).

³⁰P. Halevi and G. Hernandez-Cocoletzi, *Phys. Rev. Lett.* **48**, 1500 (1982).

³¹N. N. Akhmediev and V. V. Yatsishen, *Solid State Commun.* **27**, 357 (1978).

³²V. L. Shekhtman and O. E. Shirokbrod, *Opt. Spektrosk.* **62**, 698 (1987) [*Opt. Spectrosc. (USSR)* **62**, 414 (1987)].

³³P. M. Morse and H. Feshbach, *Methods of Theoretical Physics*, 2 vols., McGraw-Hill, New York (1953).

³⁴M. F. Bishop and A. A. Maradudin, *Phys. Rev. B* **14**, 3384 (1976).

³⁵A. Sel'kin, *Phys. Status Solidi B* **83**, 47 (1977).

- ³⁶I. B. Tampil', V. L. Shekhtman, O. E. Shirokobrod, and A. F. Yakubov, *Fiz. Tverd. Tela (Leningrad)* **31**, 69 (1989) [*Sov. Phys. Solid State* **31**, 38 (1989)].
- ³⁷S. A. Permogorov, V. V. Travnikov, and A. V. Sel'kin, *Fiz. Tverd. Tela (Leningrad)* **14**, 3642 (1972) [*Sov. Phys. Solid State* **14**, 3051 (1973)].
- ³⁸V. V. Travnikov, *Izv. Akad. Nauk SSSR Ser. Fiz.* **52**, 758 (1988).
- ³⁹V. V. Travnikov, *Pis'ma Zh. Eksp. Teor. Fiz.* **44**, 133 (1986) [*JETP*

Lett. **44**, 169 (1986)].

- ⁴⁰J. Wicksted, M. Matsushita, H. Z. Cummins, T. Shigenari, and X. Z. Lu, *Phys. Rev. B* **29**, 3350 (1984).

Translated by A. Tybulewicz